inter.noise
HAMBURG 2016

Cross-spectral Matrix Diagonal Reconstruction

Jørgen HALD[1]

[1] Brüel & Kjær SVM A/S, Denmark

ABSTRACT

In some cases, measured cross-spectral matrices (CSM's) from a microphone array will be contaminated by severe incoherent noise signals in the individual channels. A typical example is flow noise when measuring in a wind tunnel. Assuming stationary signals and performing long-time averaging, the contamination will be concentrated on the diagonal of the CSM. When the CSM is used for traditional frequency-domain beamforming, the use of the diagonal can be avoided – a technique referred to as Diagonal Removal (DR). DR is effective at suppressing the effects of the contamination, but it also has some side effects, such as underestimation of source levels. With other beamforming algorithms, such as Functional Beamforming, and in connection with acoustic holography, however, the diagonal of the CSM is needed. The present paper describes a method for removal of incoherent noise contamination from the CSM diagonal. The method formulates the problem as a Semidefinite Program, which is a convex optimization problem that can be solved very efficiently and with guaranteed convergence properties. A numerical study focuses on the question, whether the Semidefinite Program formulation will provide in all cases the desired output, i.e. the diagonal with precisely the contamination removed. Results from measurements are also presented.

Keywords: Wind noise, beamforming, diagonal removal.
I-INCE Classification of Subjects Number(s): 74.7, 74.1

1. INTRODUCTION

Microphone array measurements performed outdoor or in wind tunnels will often suffer from self-induced flow noise in the individual microphones (1). Use of windscreens can reduce the effect, but not remove it. For frequency-domain beamforming applications, averaging of a Cross Spectral Matrix (CSM) is typically first performed. If the measured flow-noise signals are (to a good approximation) independent stationary stochastic processes over the measured time interval, and if the averaging time is sufficiently long, then the flow noise will contribute almost entirely on the diagonal of the averaged CSM. Use of windscreens will reduce the noise, but the noise from one windscreen may be picked up by neighboring microphones, if the screens are not much smaller than the microphone spacing, resulting in contributions outside the CSM diagonal.

Assuming the flow-noise contributions to be concentrated on the CSM diagonal, their effect on beamforming results can be almost entirely removed by use of so-called Diagonal Removal (DR), where the use of the diagonal elements is avoided (1). This technique has a simple and robust implementation in connection with traditional frequency domain beamforming, typically Delay And Sum (DAS). Unfortunately, it also has some side effects, such as underestimation of source levels and areas with negative power in produced contour maps. With other beamforming algorithms, such as Functional Beamforming, and in connection with acoustic holography, the diagonal of the CSM is needed.

Beamforming deconvolution techniques based on use of the so-called Point Spread Function (PSF), such as Non-Negative Least Squares (2), can be implemented with DR, because the PSF can be calculated using DR. Clean-SC (3) also includes a DR procedure, which however is much more complicated, requiring for each new identified point source an iterative solution of a system of non-linear equation. In reference (4) the iterative solution procedure was found to work nicely for the strong sources, but to fail converging for the weaker sources. To overcome that limitation, the algorithm introduced in the present paper was adopted.

Dougherty (5) recently published a paper describing a method entitled Cross Spectral Matrix

[1] jorgen.hald@bksv.com

Diagonal Optimization, which uses the same idea as the method of the present paper to remove microphone self-noise contributions from the CSM diagonal: The idea is to minimize the sum of the auto-power elements on the CSM diagonal, while maintaining the matrix positive semidefinite (i.e. with non-negative eigenvalues). All off-diagonal elements remain unchanged. The present paper describes a different solution procedure making use of recent developments in Convex Optimization; see for example references (6) and (7). This allows the problem to be solved very efficiently and with guaranteed convergence properties.

The new Diagonal Reconstruction (DiRec) method is outlined in Section 2. Following that, Section 3 presents a numerical investigation of the conditions under which the new DiRec method will return a diagonal with all incoherent noise contributions removed and with nothing else removed. Results from actual measurements with flow noise are presented in Section 4. Here, a specific focus is on the importance of using sufficient averaging to concentrate the flow noise contributions on the diagonal of the CSM. Finally, Section 5 gives a summary.

2. THEORY

Let $\mathbf{C}$ be an $M\times M$ element complex Hermitian cross-spectral matrix contaminated by microphone self-noise contributions on its diagonal. We would like to add an $M\times M$ element diagonal matrix $\mathbf{D}$ with unknown non-positive diagonal elements d_m to cancel the self-noise. Arranging the unknown diagonal elements in an M-element vector $\mathbf{d}$, we write $\mathbf{D} = \mathbf{diag}\{\mathbf{d}\}$. After the determination of $\mathbf{D}$ we will replace $\mathbf{C}$ by $\mathbf{C}+\mathbf{D}$. Cancelling the self noise on the diagonal implies a minimization of the sum of the elements d_m. However, the remaining matrix $\mathbf{C}+\mathbf{D}$ must still be Hermitian, i.e. with non-negative eigenvalues. Therefore, the idea is to determine $\mathbf{d}$ as the solution to:

$$\min_{\mathbf{d}} \sum_m d_m \quad \text{subject to} \quad \mathbf{C} + \mathbf{diag}\{\mathbf{d}\} \geq 0, \tag{1}$$

where "≥ 0" for a matrix means that it is positive semidefinite. The problem (1) has the form of a Semidefinite Program, which can be solved efficiently and with guaranteed convergence properties using Convex Optimization methods, see for example reference (6).

Figure 1 shows the few lines of Matlab code needed to solve the problem (1) using the publicly available Matlab library CVX. The library can be downloaded from the website given in reference (7).

```
cvx_begin;
variable d(M);
C + diag(d,0) == hermitian_semidefinite(M);
minimize( sum(d) );
cvx_end;
```

Figure 1 – CVX Matlab code for performing DiRec.

An important question is whether the above solution procedure will always provide output with exactly the self-noise removed from the diagonal. The minimization in (1) will proceed until one of the eigenvalues of $\mathbf{C}+\mathbf{D}$ reaches zero, showing that too much will be removed, if the desired matrix has only positive eigenvalues. The following section presents some numerical simulations to investigate that issue. It turns out that an "exact" solution is obtained, if a small minimum number of eigenvalues of the desired matrix are equal zero. The errors resulting from a class of decaying eigenvalue distributions are also investigated.

3. INVESTIGATION BASED ON SYNTHESIZED CROSS-SPECTRAL MATRICES

The algorithm was tested by synthesis of $M\times M$ element Hermitian cross-spectral matrices from K random rank-1 matrices, $K \leq M$:

$$\widetilde{\mathbf{C}} = \sum_{k=1}^{K} \mathbf{p}_k \mathbf{p}_k^H \ . \tag{2}$$

Here, H represents conjugate transpose, and the real and imaginary parts of each element in the $M\times 1$ vectors $\mathbf{p}_k$ are generated as random numbers with zero mean and standard deviation equal to 1. The resulting matrix $\widetilde{\mathbf{C}}$ will have a set of K non-zero eigenvalues covering a wide range. To shape the eigenvalue spectrum, a singular value decomposition was first made:

$$\widetilde{\mathbf{C}} = \mathbf{U}\widetilde{\mathbf{S}}\mathbf{V}^H, \tag{3}$$

followed by a scaling of the K non-zero singular values in $\tilde{\mathbf{S}}$ to get the matrix $\mathbf{S}_0$, which is then used to obtain the modified cross-spectral matrix $\mathbf{C}_0$ with shaped eigenvalue spectrum:

$$\mathbf{C}_0 = \mathbf{U}\mathbf{S}_0\mathbf{V}^H. \tag{4}$$

This matrix $\mathbf{C}_0$ is used as the target to be recovered from a matrix $\mathbf{C}$ with noise added on its diagonal:

$$\mathbf{C} = \mathbf{C}_0 + \mathbf{diag}\{\mathbf{n}\}, \tag{5}$$

$\mathbf{n}$ being a vector of squared, suitably scaled, random numbers. Ideally, the method of Section 2 should be able remove the added noise, i.e. provide $\mathbf{d} = -\mathbf{n}$.

Section 3.1 investigates the error in the case, where the matrix $\mathbf{C}_0$ has a variable number of equal, non-zero eigenvalues (the rest being equal to zero), while Section 3.2 investigates the case of a decaying eigenvalue spectrum with none of them equal to zero.

3.1 Varying number of equal, non-zero eigenvalues

In this case, the largest singular value $\tilde{S}_{max}$ in $\tilde{\mathbf{S}}$ was identified, and the singular values $S_{0,m}$ of $\mathbf{S}_0$ were then set as:

$$\begin{aligned} S_{0,m} &= \tilde{S}_{max} \quad m = 1, 2, \ldots, K, \\ S_{0,m} &= 0 \qquad m = K+1,\ K+2, \ldots, M. \end{aligned} \tag{6}$$

Based on $\mathbf{S}_0$, the matrix $\mathbf{C}_0$ could be computed using Eq. (4). The elements of the noise vector $\mathbf{n}$ were initially generated as squared random variables with zero mean and standard deviation 1. Subsequently they were scaled to have standard deviation a chosen number of decibel, X, higher than the average $\mathbf{C}_0$ auto-power. Finally, $\mathbf{C}$ could be generated through application of Eq. (5).

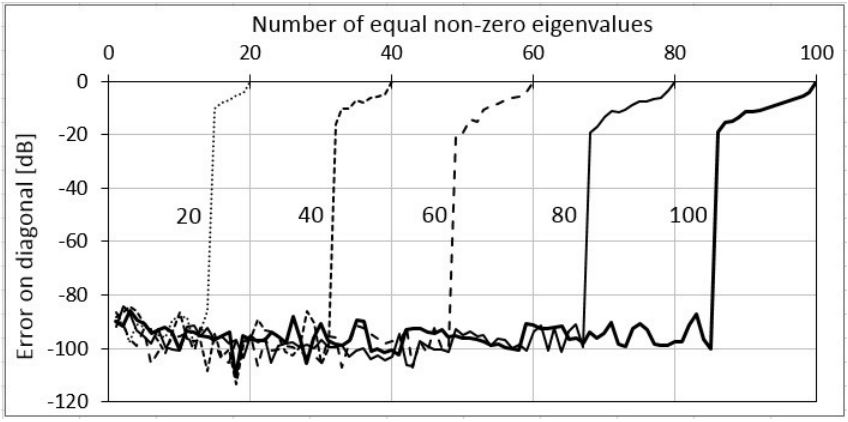

Figure 2 – For five different arrays with 20, 40, 60, 80 and 100 microphones, the reconstruction error *Err* is shown as a function of the number of equal, non-zero CSM eigenvalues.

After the solution of the DiRec problem (1), the deviation from the ideal solution $\mathbf{d} = -\mathbf{n}$ was quantified by the error function:

$$Err = 10 * \log 10\left[\frac{\sum_{m=1}^{M}|d_m + n_m|}{\sum_{m=1}^{M} C_{0,m,m}}\right], \tag{7}$$

where d_m are the elements of $\mathbf{d}$, n_m are the elements of $\mathbf{n}$, and $C_{0,m,m}$ are the diagonal elements of $\mathbf{C}_0$. Figure 2 shows this relative error as a function of the number K of equal, non-zero eigenvalues for 5 different values of the matrix dimension M used as annotation at the curves: M = 20, 40, 60, 80 and 100. In this case, the level X of the added noise was set to be 40 dB above the average level on the diagonal of $\mathbf{C}_0$, but several levels were tested with almost identical result: X = 0, 20, 40 dB. Thus, apparently it is not the level of the added noise that sets the accuracy, but rather the eigenvalue spectrum of the desired matrix $\mathbf{C}_0$. Based on a series of simulations and results like those in Figure 2 it was found that effectively an exact noise subtraction can be performed, when the number K of equal non-zero eigenvalues does not exceed a value $K_{\max}$ given as:

$$K_{max}(M) = M - \sqrt{2.5 * M}. \tag{8}$$

Close to the point, where K exceeds $K_{\max}$, the relative error increases steeply to be in the range between

-20 and -10 dB, and after that point it increases smoothly to be 0 dB at $K = M$. As mentioned above, the method cannot handle accurately the situation, where all eigenvalues are positive. Intuitively one might think that the method should work perfectly as long as $\mathbf{C}_0$ had just one eigenvalue equal to zero. The reason why a number of eigenvalues must equal zero is not known. A guess could be finite precision in the number handling, but it remains as an interesting open question.

3.2 Decaying eigenvalue distribution

In practical applications, the desired CSM $\mathbf{C}_0$ will normally have a more or less smoothly decaying spectrum of eigenvalues. Here, we will consider spectra of the form shown in Figure 3, which are synthesized from the formula:

$$S_{0,m} = e^{-\alpha m^2/M}, \quad m = 1,2,\ldots,M, \tag{9}$$

with α set to produce a specific attenuation A in decibel at $m = M$. In the case of Figure 3 the attenuation is $A = 40$ dB, which is also the range covered by the eigenvalue spectrum.

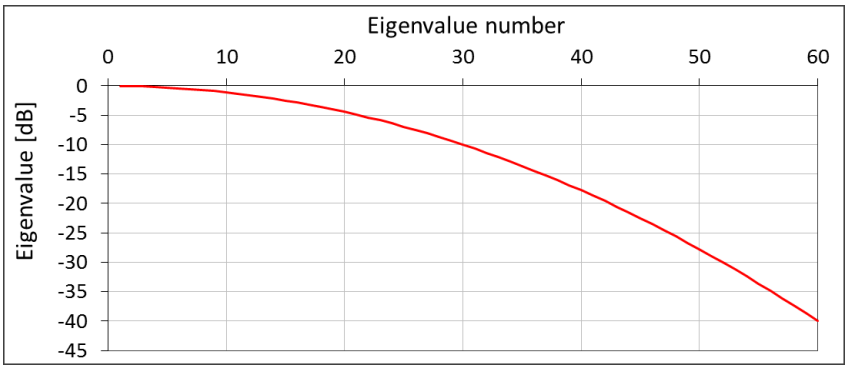

Figure 3 – Simulated CSM eigenvalue distribution with 40 dB range for a 60-element array.

After calculation of $\mathbf{C}_0$ by Eq. (4), the noise vector $\mathbf{n}$ was calculated using the same procedure as described in Section 3.1. For this, the level X of the noise relative to the average auto-power on the diagonal of $\mathbf{C}_0$ had to be chosen. Again, it turned out that the errors were to a good approximation independent of the noise level, depending almost entirely on the eigenvalue spectrum. Figure 4 shows the relative noise removal error, calculated using Eq. (7), as a function of the eigenvalue range A for an array with $M = 60$ microphones. The relative noise level was again $X = 40$ dB, i.e. the noise was 40 dB higher than the average auto-power on the diagonal of $\mathbf{C}_0$. Except for the highest values of A, Figure 4 shows that with axes in decibel the relative noise removal error is close to a linear function of A. For the chosen eigenvalue-spectrum shape, the relation is Err[dB] ≈ -0.65 * A[dB]. A similar relation was true for other values of M, the slope of the linear relation increasing slowly with M.

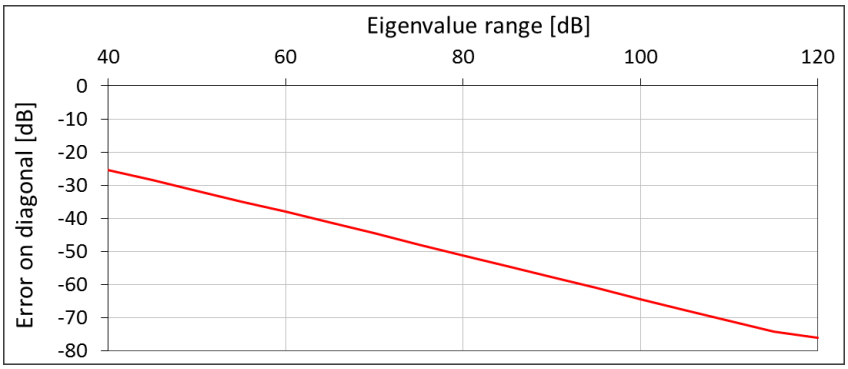

Figure 4 – Reconstruction error *Err* for a 60-element array with CSM eigenvalue distribution of the type shown in Figure 3. The eigenvalue range A is on the x-axis.

An interpretation of the results in this section and in Section 3.1 is that solution of Eq. (1) will very effectively remove noise added on the diagonal of the CSM, but depending on the eigenvalue spectrum it will also remove/modify some of the desired diagonal. If a sufficient number of eigenvalues are zero or very small, then the introduced error is negligible.

4. MEASUREMENTS

A series of measurements were performed on a small loudspeaker excited by broadband random noise. Each configuration was measured with and without flow incident on the array. Since the speaker signal and the flow-induced noise in the microphones are mutually incoherent, the measured CSM will ideally be the sum of their contributions: $\mathbf{CSM}_{\text{total}} = \mathbf{CSM}_{\text{speaker}} + \mathbf{CSM}_{\text{flow}}$. Due to finite averaging time, though, the equation will hold only approximately. With the first and the last of the three matrices measured, the flow noise contribution $\mathbf{CSM}_{\text{flow}}$ can be calculated. The DiRec method relies on that matrix being close to diagonal, i.e. with the measured coherence between all flow-noise signals close to zero. One thing to be aware of is possible large errors in the elements of $\mathbf{CSM}_{\text{flow}}$ because it is obtained as a difference between two non-simultaneously measured matrices. It could have been measured directly, but that was not done.

Two different flow conditions were measured, since they provide different challenges: 1) Flow with large-scale turbulence. 2) Approximate laminar flow concentrated on an small array section.

4.1 Turbulent flow

Figure 5 – Picture of the setup with array (right), source (left) and flow-outlet nozzle (bottom).

A series of measurements were taken with a 36-element pseudo-random array on a Brüel & Kjaer Mouth Simulator Type 4227 excited by white random noise. Figure 5 shows the setup with the 45 cm diameter array at 40 cm distance from the source and with a flow-outlet nozzle entering at the bottom. The nozzle emitted a flow-beam towards the array center, but due to the quite long distance, the microphones were exposed to a diverged beam with turbulent rather than laminar flow. Despite the long distance, the flow speed was very inhomogeneous across the array. For a set of different excitation levels of the source, 20 sec recordings with 32768 Hz sampling frequency were taken with and without the flow. Using a 200-line FFT for cross-spectral averaging, 2559 averages could be achieved. Only results for a single selected source excitation level will be presented below.

Figure 6 shows the 36 auto-power spectra from the measurement with no flow, while the corresponding spectra with flow are shown in Figure 7. Clearly, the flow adds some strong low-frequency noise, the level of which varies between the microphones and decreases with increasing frequency. The added noise is strong at the center of the flow beam, and it decreases away from that point. Inspection of the flow profile, just by holding a hand in it, indicated a reasonably laminar flow at the core, but otherwise a lot of large-scale turbulence. This has been confirmed by visual inspection of the recorded time signals and by listening to these signals. The microphones furthest away from the core flow have almost no added flow noise.

Based on the measurements with and without flow, the CSM of the flow noise, $\mathbf{CSM}_{\text{flow}}$, was

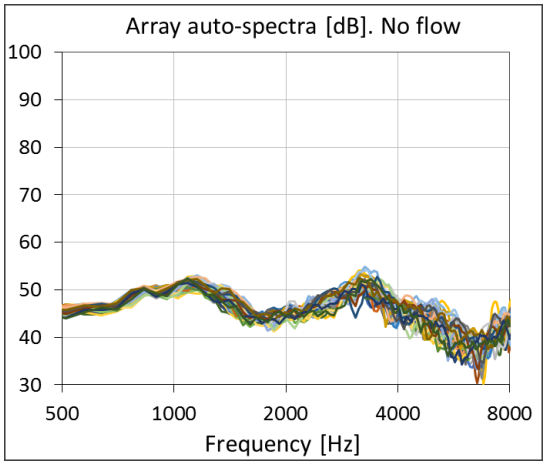

Figure 6 – Auto-power spectra. No flow.

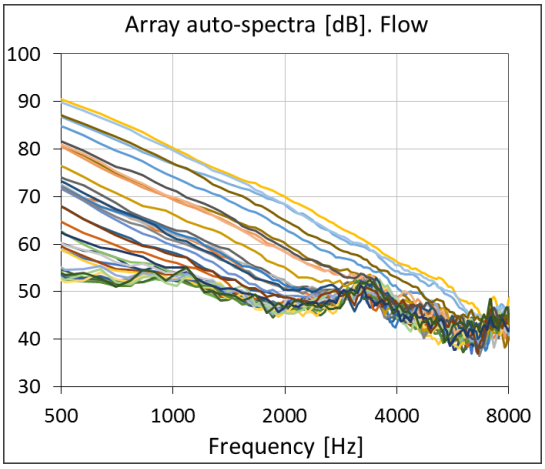

Figure 7 – Auto-power spectra. Flow.

estimated as described above. The degree to which $\mathbf{CSM}_{\text{flow}}$ is diagonal could be represented in several ways. Here, a representation based on the squared coherence function

$$\gamma_{i,j}^2 = \frac{\left|CSM_{i,j}\right|^2}{CSM_{i,i} \cdot CSM_{j,j}} \tag{10}$$

between microphone signals i and j has been chosen. Only, instead of looking at coherences between single microphone pairs, an average coherence for the full matrix is calculated using the expression:

$$\bar{\gamma}^2 \equiv \frac{\sum_{i \neq j} \left|CSM_{i,j}\right|^2}{\sum_{i \neq j} \left|CSM_{i,i}\right| \cdot \left|CSM_{j,j}\right|}. \tag{11}$$

Clearly, for a diagonal matrix that average coherence will equal zero. Direct application of Eq. (10) to the matrix $\mathbf{CSM}_{\text{flow}}$ gave in some cases large errors, because the matrix is calculated as the difference between two non-simultaneously measured CSM's. The formula (11) for the average coherence is, however, very robust.

Figure 8 shows the average coherence function $\bar{\gamma}$ for the flow contribution $\mathbf{CSM}_{\text{flow}}$ over the frequency range from 500 Hz to 8 kHz. Up to around 2 kHz, only a low level of coherence around 0.02 is found, which can be explained as being entirely due to the limited number of averages: Assuming zero coherence between two stationary random signals x and y, the residual coherence γ_{xy} after N averages can be shown to be $1/\sqrt{N}$, see for example reference (8). With 2559 averages, this residual coherence will be 0.020, which fits perfectly with the result in Figure 8 below 2 kHz. Above 3 kHz, Figure 8 shows an average coherence that increases up to approximately 0.7 at 8 kHz. The first idea was that perhaps the diagonal elements in $\mathbf{CSM}_{\text{flow}}$ were too small to be determined with sufficient accuracy as the difference between elements of $\mathbf{CSM}_{\text{total}}$ and $\mathbf{CSM}_{\text{speaker}}$. However, the same type of result was obtained from measurements with lower speaker excitation levels, where the flow contributions were higher than the speaker contributions. Another possible explanation could be the large-scale turbulence, where microphones are hit by flow bursts at irregular time intervals. To investigate that, another series of measurements was conducted as described in the following section.

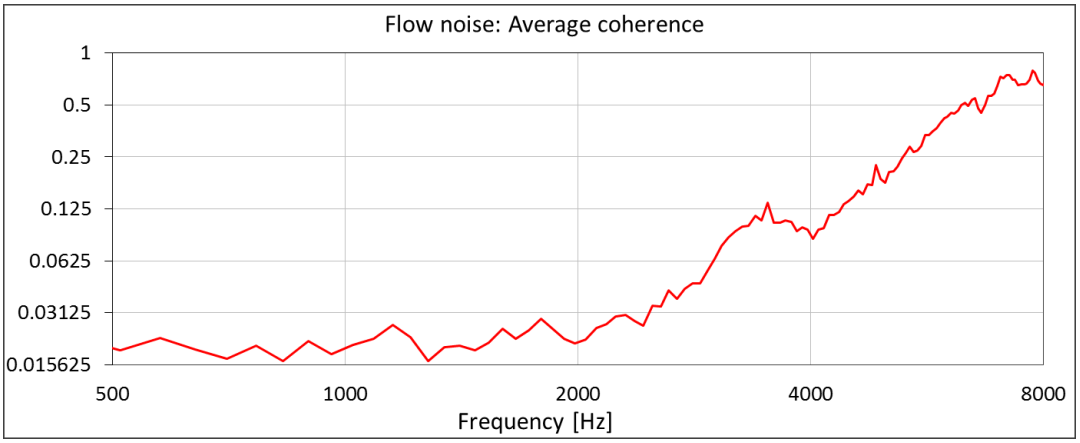

Figure 8 – Average coherence for the measured flow-noise CSM.

As mentioned previously, the DiRec algorithm relies on the flow noise contributions being concentrated on the diagonal of the CSM. Significant off-diagonal elements in $\mathbf{CSM}_{\text{flow}}$, indicated by rather high average coherence in Figure 8, will force the algorithm to retain some flow-noise related contributions on the diagonal of the CSM in order to retain the matrix positive semidefinite.

Figure 9 shows the achieved reduction in decibel of the flow-noise-related auto-power sum (the sum of the diagonal elements in $\mathbf{CSM}_{\text{flow}}$), when applying the DiRec algorithm to the matrix $\mathbf{CSM}_{\text{total}}$: The speaker contribution $\mathbf{CSM}_{\text{speaker}}$ was subtracted from the $\mathbf{CSM}_{\text{total}}$ before and after application of DiRec to $\mathbf{CSM}_{\text{total}}$ to get the flow-noise CSM's before and after. Figure 9 shows the ratio between the auto-power sums for these two flow-noise CSM's. Up to around 2 kHz a reduction around 10 dB is obtained, but from 4 kHz up to 8 kHz it decreases to be close to 0 dB. That decrease is due to the larger off-diagonal elements in $\mathbf{CSM}_{\text{flow}}$, represented by the higher measured average coherence in Figure 8.

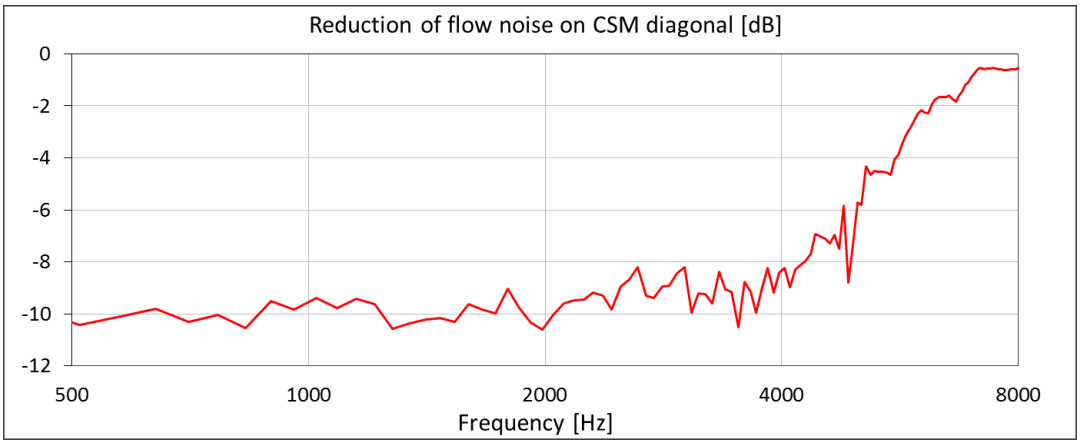

Figure 9 – Reduction of flow-noise auto-power sum on the CSM diagonal obtained using the DiRec method of Section 2.

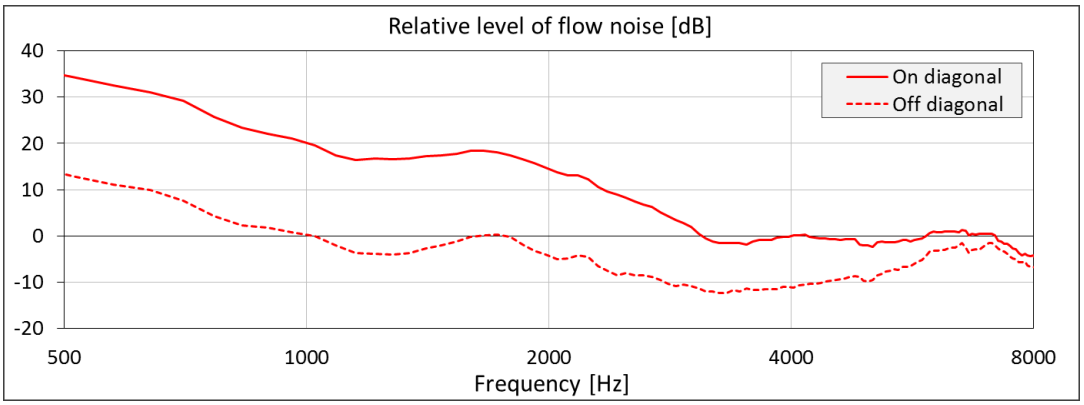

Figure 10 – Average element sizes in $\mathbf{CSM}_{\text{flow}}$ relative to average element sizes in $\mathbf{CSM}_{\text{speaker}}$.

Thus, remaining flow-noise related off-diagonal contributions in $\mathbf{CSM}_{\text{total}}$ will limit the reduction of the flow-noise auto-power contributions that can be achieved by use of the DiRec algorithm. The degree to which this will be visible in beamformed maps depends on the level of the flow noise relative to the level of the source signal of interest. Figure 10 shows the average level differences between the elements of $\mathbf{CSM}_{\text{flow}}$ and $\mathbf{CSM}_{\text{speaker}}$. Elements on the CSM diagonal (solid red) and off-diagonal elements (dashed red) are considered separately. Considering for example the off-diagonal elements, the average of absolute values is calculated for $\mathbf{CSM}_{\text{flow}}$, the same is done for $\mathbf{CSM}_{\text{speaker}}$, and the level difference between the two averages is plotted.

Between 6 and 8 kHz the average flow-noise auto-power is approximately equal to the average speaker auto-power. Due to the measured high coherence of the flow noise in that range, the DiRec algorithm can reduce the flow-noise auto-power sum by only between 0 and 3 dB, see Figure 9. The remaining auto-power, together with the significant flow-noise off-diagonal elements (observed in Figure 10), leads to the poor flow-noise suppression by DiRec seen in the DAS beamforming map for the 6.3 kHz 1/3-octave band in Figure 11. Beamforming was here performed on narrow-band CSM's, and the output was synthesized into 1/3-octave bands.

Each row in Figure 11 represents a given 1/3-octave band with the same color scale used in all four plots. The first (leftmost) three columns were obtained from the measurement with flow, whereas the fourth and last column is from the corresponding measurement without flow. Column 1 represents use of the basic DAS algorithm, in column 2 the DiRec algorithm has been applied before DAS, and in column 3 the traditional diagonal removal (DR) method has been used.

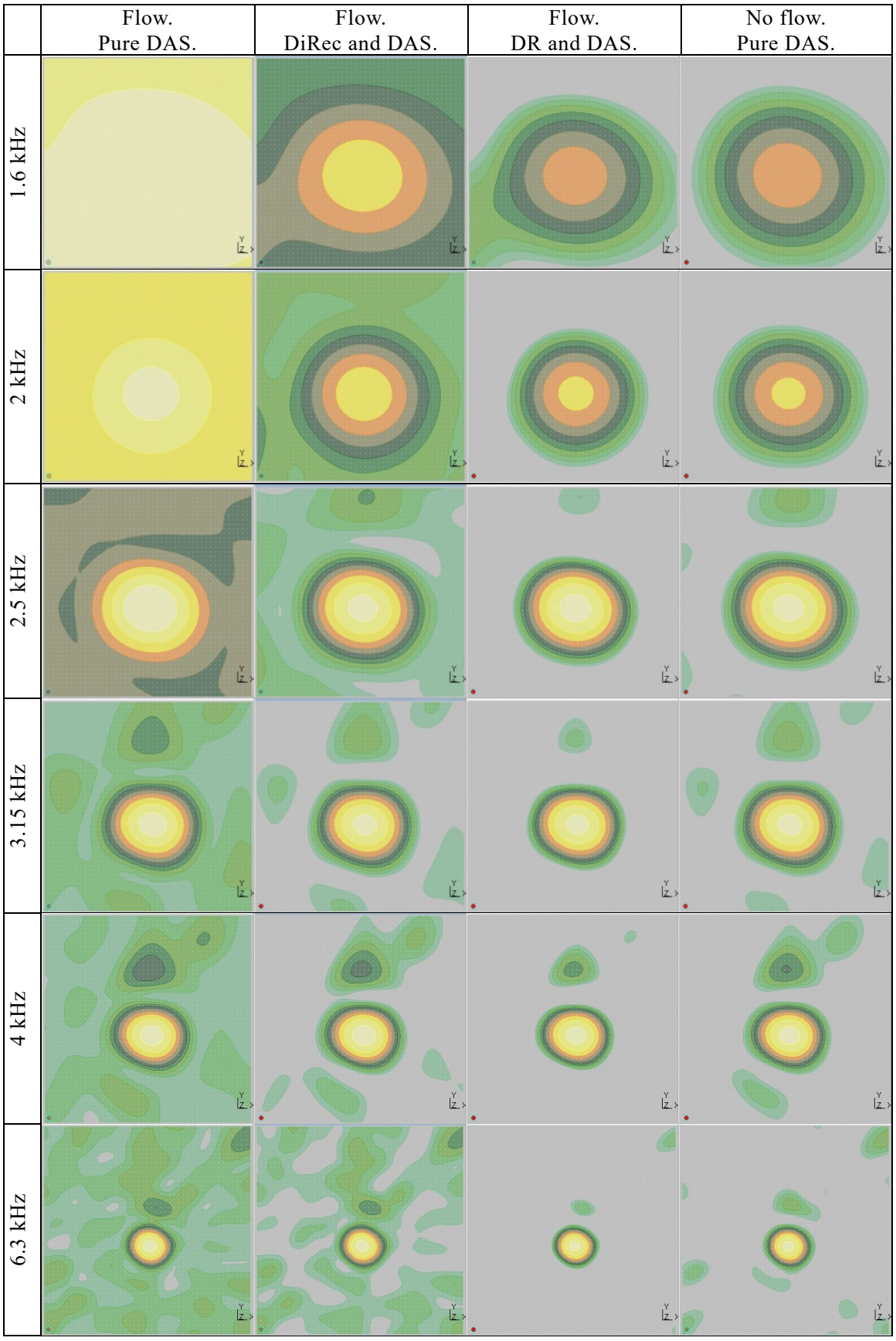

Figure 11 – DAS beamforming results in synthesized 1/3-octave bands. All plots in a row use the same color scale. Display range is 15 dB, corresponding to 1.5 dB between colors.

Looking at the leftmost column, the flow noise almost completely hides the source of interest up to around 2 kHz, and from that point, the source gradually becomes clearer up to 3.15 kHz. This agrees nicely with the variation of the flow noise contribution on the CSM diagonal represented by the solid curve in Figure 10. Use of the traditional DR provides a very good suppression of the flow noise effects, even at 1.6 and 2 kHz, where the flow noise has a significant contribution to the CSM off-diagonal elements. In comparison, the suppression obtained with the DiRec method is not as good, although it also provides a very good improvement compared to doing nothing (leftmost column). The reason is as already explained that the algorithm is forced to retain flow-noise related diagonal components corresponding to the off-diagonal flow-noise contributions in order to maintain the CSM positive semidefinite. These retained diagonal components will increase the flow-noise effects seen in DAS maps. At 3.15 and 4 kHz one can notice that DiRec recovers the sidelobe pattern obtained when pure DAS is applied to the measurement with no flow. Use of traditional DR does the well-known sidelobe reduction. At both 3.15 and 4 kHz, Figure 10 shows a significant flow-noise contribution on the diagonal, but the measured flow-noise coherence, shown in Figure 9, is sufficiently low that the DiRec algorithm can perform a good suppression of the flow noise. Below the 3.15 kHz 1/3-octave band there is also a low measured flow-noise coherence, but the flow-noise auto-power contribution is becoming too strong to be effectively suppressed.

4.2 Approximate laminar flow over array section

Figure 12 – Picture of the setup with array (right), source (left) and flow-beam hose (bottom right).

As described in the above section, the measured high flow-noise coherence above 4 kHz in Figure 9 was assumed to be caused by large-scale turbulence. To further investigate that, a series of measurements were taken with the flow outlet moved very close to a bottom section of a small 30-channel array with the microphones flush mounted in a plate, see Figure 12. The diameter of the array was 30 cm, and the measurement distance was again 40 cm. As a result, the lowest 6-7 microphones were exposed to strong, approximately laminar flow, with much lower flow speed at the remaining microphones. This was checked by putting a hand in the flow and by listening to the recorded signals. For a set of different excitation levels of the source, 30 sec recordings with 32768 Hz sampling frequency were taken with and without the flow. Only results for one of the source levels will be presented here. The 30 second recordings were used to calculate CSM's based on 3839 averages with a 200-line FFT.

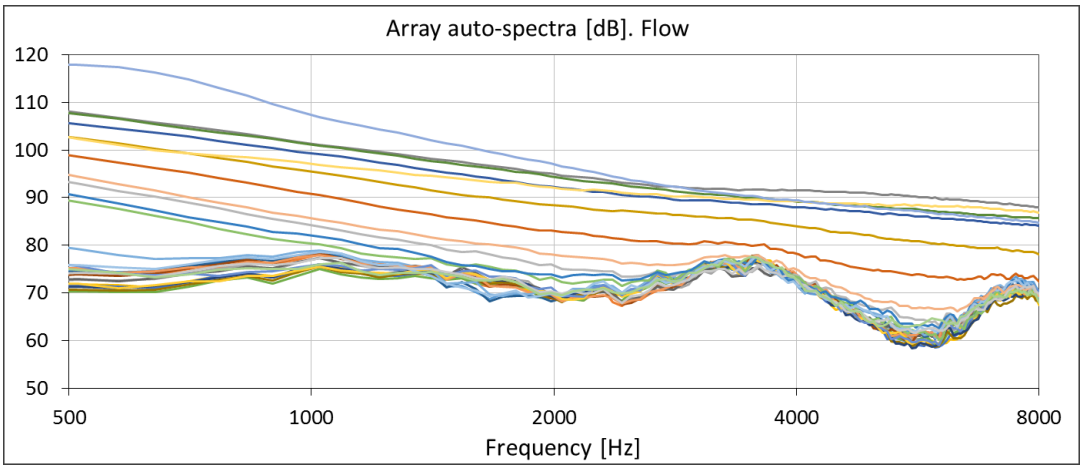

Figure 13 – Auto-power spectra. Flow.

Figure 13 shows the 30 auto-power spectra from the measurement with flow. The 6-7 microphones exposed to strong flow are easily identified. Figure 14 shows the average coherence $\bar{\gamma}$ obtained by application of Eq. (11) to the estimated flow-noise CSM, exactly like the results in Figure 8 were

obtained. Above 1.2 kHz the average coherence is low and fluctuates around 0.016, which corresponds precisely to the residual coherence between two truly incoherent signals after 3839 averages. Thus, for the present case of strong, approximately laminar flow over a subset of the microphone, the high average coherence appearing in Figure 8 above 3 kHz has disappeared. This could indicate the coherence increase in Figure 8 being due to large-scale turbulence. A small increase in the average coherence is seen in Figure 14 below 1.2 kHz. The reason is unknown, but it might be related to the extraordinarily high signal level measured by a single microphone at these low frequencies, see Figure 13. That microphone was the one closest to the flow-outlet nozzle.

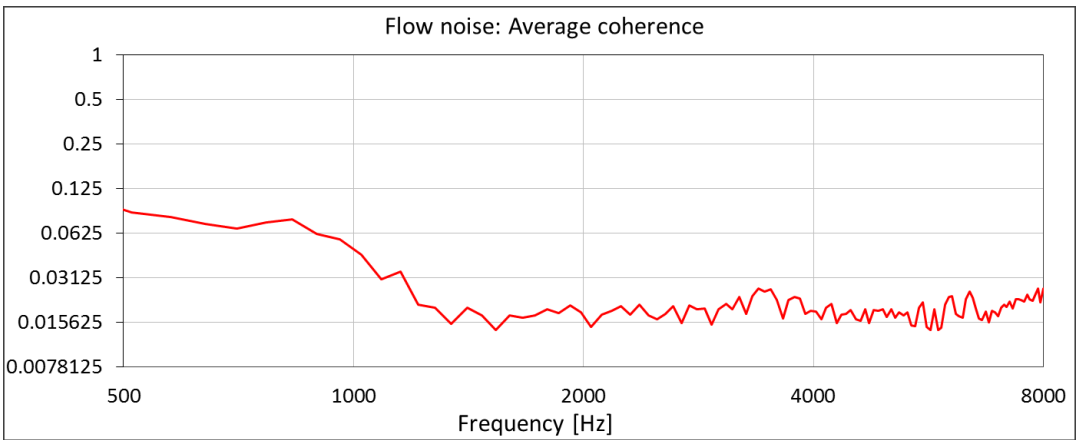

Figure 14 – Average coherence for the measured flow-noise CSM.

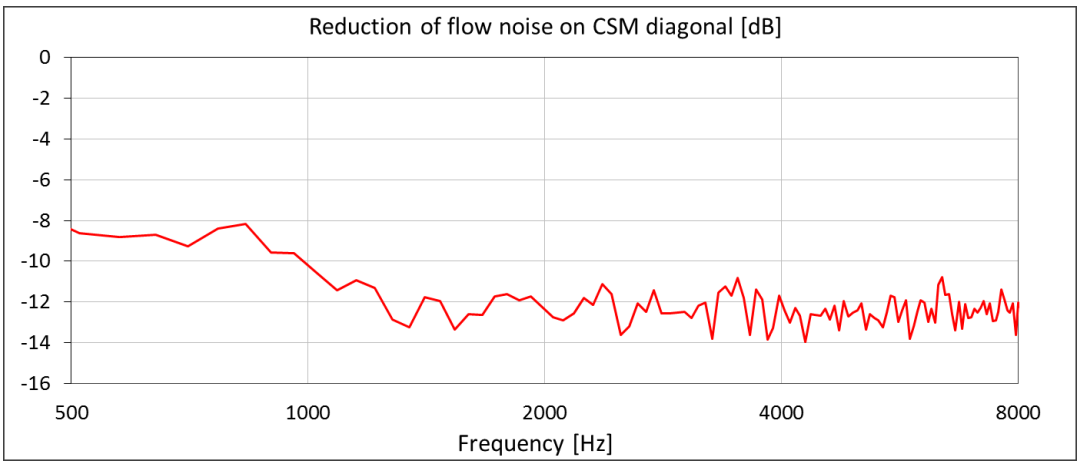

Figure 15 – Reduction of flow-noise auto-power on the CSM diagonal obtained using the DiRec method of Section 2.

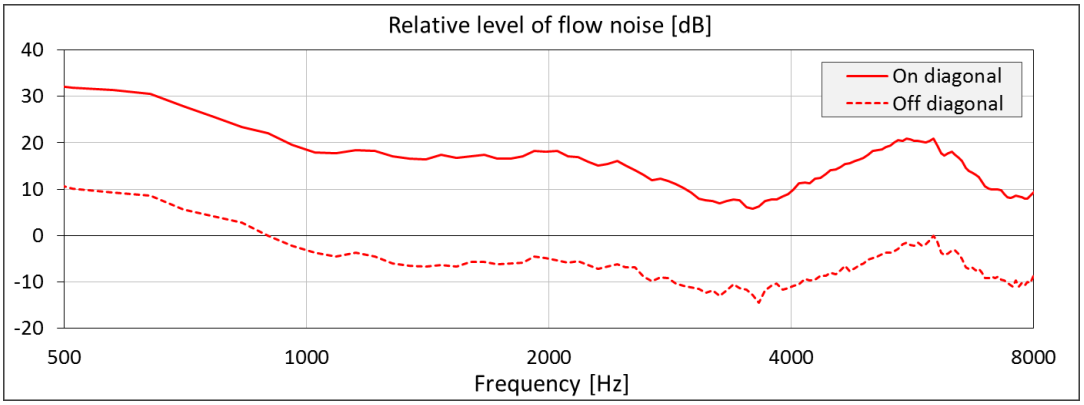

Figure 16 – Average element sizes in $\mathbf{CSM}_{\text{flow}}$ relative to average element sizes in $\mathbf{CSM}_{\text{speaker}}$.

Figure 15 shows the reduction in flow-noise auto-power provided by the DiRec algorithm. Notice

the very close match with the average flow-noise coherence $\bar{\gamma}$ in Figure 14. Actually, the reduction in flow-noise auto-power is very close to $7 \cdot \log10(\bar{\gamma})$ decibel over the full frequency range. Above 1.2 kHz we have further $\bar{\gamma} \approx 1/\sqrt{N}$, where N is the number of averages used in the CSM calculation.

Figure 16 shows the average level-differences between the elements of $\mathbf{CSM}_{\text{flow}}$ and $\mathbf{CSM}_{\text{speaker}}$ on and off the diagonal. The average flow-noise auto power is seen to be higher than the average speaker auto-power over the full frequency range, while the average flow-noise cross-power is a bit lower than the average speaker cross-power at all frequencies above 1 kHz. DiRec will attenuate the flow-noise auto-power spectrum by the decibel values shown in Figure 15. This will bring the flow-noise auto-power below the speaker auto-power only in a frequency band around and somewhat below 4 kHz plus in a band near 8 kHz.

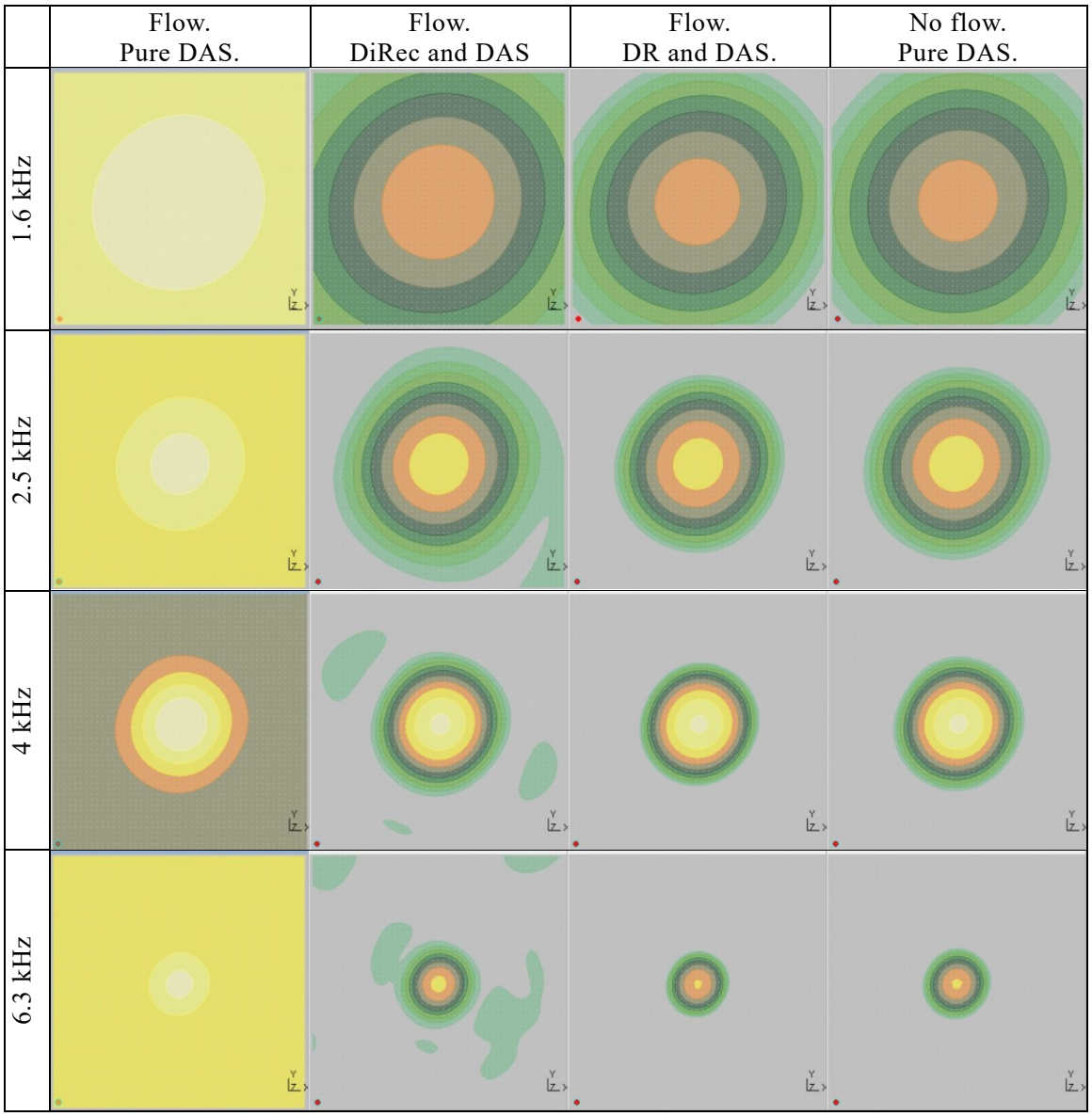

Figure 17 – DAS beamforming results in synthesized 1/3-octave bands. All plots in a row use the same color scale. Display range is 15 dB, corresponding to 1.5 dB between colors.

These observations agree quite well with the DAS beamforming maps presented in Figure 17. In the 4 kHz 1/3-octave band, DiRec provides a map very close to the map obtained from the measurement without flow. In the other 1/3-octave bands there are slightly larger remaining effects of the flow noise. Again, the classical DR method is very good at minimizing the flow-noise effects in the DAS maps, even when there are significant off-diagonal contributions from the flow noise in the CSM. Such a high off-diagonal contribution is seen in Figure 16 in a band around 6.3 kHz, but the DAS results in Figure

17 show no flow-noise effects in the 6.3 kHz 1/3-octave band, when DR is used in connection with the measurement with flow.

5. Summary

The subject of the paper has been methods to reduce the impact on array-processing results of incoherent noise in individual measurement channels, typically flow noise in connection with measurements in wind tunnels or outdoors. Diagonal Removal (DR) is an established technique for noise reduction with conventional frequency-domain Delay And Sum beamforming, avoiding completely the use of the diagonal of the cross-spectral matrix (CSM). However, DR also has some limitations and with some array processing methods, it does not apply. The present paper has described a method called Diagonal Reconstruction (DiRec) to remove the incoherent noise contributions from the diagonal of the CSM. The idea is to minimize to sum of the CSM diagonal elements, while leaving all off-diagonal elements unchanged, and while keeping the CSM positive semidefinite. The problem has the form of a so-called Semidefinite Program, which can be solved very efficiently and with guaranteed convergence properties using Convex Optimization methods.

The properties and limitations of the method were first investigated by applying it to computer synthesized CSM's with noise added on the diagonal. It turned out that for CSM's with more than $\sim\sqrt{2.5 * M}$ eigenvalues equal to zero, M being the number of microphones, DiRec is accurate within the numerical accuracy almost independent of the level of the noise added on the diagonal. For CSM's with eigenvalues decaying smoothly following an assumed form, the reconstruction accuracy was shown to be very good – also virtually independent of the level of the noise added on the diagonal.

Measurements have been performed on a small loudspeaker with the array exposed to airflow. Two types of airflow were tested: 1) With the flow-outlet nozzle at some quite long distance, the array was exposed to mainly large-scale turbulence. 2) With the nozzle close to a small group of the array microphones, these microphones were exposed to approximately laminar flow. In both cases, the achievable noise reduction on the CSM diagonal was shown to be limited by off-diagonal contributions from the flow noise. Even with perfectly incoherent flow-noise signals in the individual channels there will be residual off-diagonal contributions due to finite averaging time. These off-diagonal contributions will limit the noise reduction on the diagonal. For measurements with large-scale turbulence at the array, a particular problem with large flow-noise-related off-diagonal elements was observed at high frequencies. More investigation would be needed to conclude that the reason is large-scale turbulence.

REFERENCES

1. Dougherty R.P. Beamforming in Acoustic Testing. Aeroacoustic Testing. Edited by T.J. Mueller; Springer; Berlin; 2002; pp. 93-96.
2. Ehrenfried, K. and Koop, L. A comparison of iterative deconvolution algorithms for the mapping of acoustic sources. Proc 12th AIAA/CEAS Aeroacoustics Conference (27th AIAA Aeroacoustics Conference); 2006; Paper no. AIAA 2006-2711.
3. Sijtsma P. CLEAN Based on Spatial Source Coherence. Proc 13th AIAA/CEAS Aeroacoustics Conference (28th AIAA Aeroacoustics Conference); 2007; Paper no. AIAA 2007-3436.
4. Hald J. Mapping of contributions from car-exterior aerodynamic sources to an in-cabin reference signal using Clean-SC. Proc INTER-NOISE 16; 21-24 August 2016; Hamburg; Germany 2016.
5. Dougherty R.P. Cross Spectral Matrix Diagonal Optimization. Proc 6th Berlin Beamforming Conference; 31st February to 1st March 2016; Berlin; Germany; 2016; Paper no. BeBeC-2016-S2.
6. Vandenberghe L. and Boyd S. Semidefinite Programming. SIAM Review; Vol. 38, No. 1, pp. 49-95; March 1996.
7. Grant M. and Boyd S. CVX: Matlab software for disciplined convex programming, version 2.1. http://cvxr.com/cvx, 2014.
8. Bendat S.B. and Piersol A.G. Engineering Applications of Correlation and Spectral Analysis. John Wiley & Sons; 1980.